

Exponential entanglement advantage in sensing correlated noise

Yu-Xin Wang (王语馨)^{1,*} Jacob Bringewatt,^{1,2,3} Alireza Seif,⁴
 Anthony J. Brady,^{1,3} Changhun Oh,⁵ and Alexey V. Gorshkov^{1,3}

¹*Joint Center for Quantum Information and Computer Science,
 NIST/University of Maryland, College Park, MD, 20742, USA*

²*Department of Physics, Harvard University, Cambridge, MA 02138 USA*

³*Joint Quantum Institute, NIST/University of Maryland, College Park, MD, 20742, USA*

⁴*IBM Quantum, IBM T.J. Watson Research Center, Yorktown Heights, NY 10598, USA*

⁵*Department of Physics, Korea Advanced Institute of Science and Technology, Daejeon 34141, Korea*

In this work, we propose a new form of exponential quantum advantage in the context of sensing correlated noise. Specifically, we focus on the problem of estimating parameters associated with Lindblad dephasing dynamics, and show that entanglement can lead to an exponential enhancement in the sensitivity (as quantified via quantum Fisher information of the sensor state) for estimating a small parameter characterizing the deviation of system Lindbladians from a class of maximally correlated dephasing dynamics. This result stands in stark contrast with previously studied scenarios of sensing uncorrelated dephasing noise, where one can prove that entanglement does not lead to an advantage in the signal-to-noise ratio. Our work thus opens a novel pathway towards achieving entanglement-based sensing advantage, which may find applications in characterizing decoherence dynamics of near-term quantum devices. Further, our approach provides a potential quantum-enhanced probe of many-body correlated phases by measuring noise generated by a sensing target. We also discuss realization of our protocol using near-term quantum hardware.

Introduction.—Quantum sensing is one of the most promising applications of near-term quantum systems [1–4], with experimental implementations of, e.g., quantum phase estimation [5–9], as well as precision measurements of time [3, 10, 11], mechanical motion [12], electric [13, 14], magnetic [15, 16], and gravitational fields [17]. In this context, understanding whether quantum entanglement provides an advantage in estimating an unknown physical quantity is a question of both fundamental importance and tremendous practical interest. Such entanglement-enabled improvement is typically expressed in terms of the asymptotic scaling of the measurement signal-to-noise ratio (SNR) with respect to resource constraints such as the number of atoms used and/or the total interrogation time. For example, for the prototypical example of sensing an unknown parameter ξ coupled to a Hamiltonian $\hat{H} = \xi \sum_{\ell=1}^N \hat{Z}_{\ell}$, the optimal strategy is to use the Greenberger–Horne–Zeilinger (GHZ) state, which leads to a \sqrt{N} entanglement advantage in estimating ξ . This is known as the Heisenberg limit [18].

However, realistic quantum systems are prone to unwanted environmental noise and decoherence, limiting the performance of quantum sensors in practice. More specifically, no quantum advantage survives in the $N \rightarrow \infty$ asymptotic limit when the sen-

sor is subject to uncorrelated Markovian dephasing noise [19–23]. In the presence of certain types of spatial or temporal correlations, however, entanglement advantage can survive [24–26]. Intriguingly, dissipative dynamics also give rise to a new sensing paradigm of environmental noise estimation [27–29], which is completely distinct from the standard Hamiltonian case. While one can prove that no entanglement advantage is present in the case of sensing independent dephasing noise [30], whether entanglement helps in sensing more general correlated noise processes remains an open question.

In this work, we answer this question positively, by proposing a class of protocols that lead to an entanglement advantage in estimating properties of near maximally-correlated Markovian dephasing noise. We first illustrate the basic mechanism of the new entanglement enhancement using a 2-qubit example. We then discuss its generalization to multiqubit systems and show that in this setting there can be an *exponential* entanglement advantage in the SNR. Our protocol enables the measurement of the two-point correlation functions of a sensing target, which can be used to design novel quantum-enhanced probes to study interacting many-body quantum systems. We conclude with a discussion of experimental implementation.

Setup: Lindbladian sensing.—Let us consider a quantum sensor consisting of N qubits that undergoes dynamics described by a Lindbladian \mathcal{L}_{ξ} parametrized by parameter ξ : $(d\hat{\rho}/dt) = \mathcal{L}_{\xi}\hat{\rho}$. While

* yxwang.physics@outlook.com

the mechanism discussed here for realizing quantum advantage is general and can be applied to non-Markovian and/or multi-axis noise, for concreteness we focus on sensing Markovian pure-dephasing noise, so that we have

$$\mathcal{L}_\xi[C(\xi)]\hat{\rho} = \frac{\gamma}{2} \sum_{j,\ell=1}^N C_{j\ell}(\xi) \left(\hat{Z}_\ell \hat{\rho} \hat{Z}_j - \frac{\{\hat{Z}_j \hat{Z}_\ell, \hat{\rho}\}}{2} \right), \quad (1)$$

where γ is a constant characterizing the overall decay time scale, and $C_{j\ell}(\xi)$ are matrix elements of a positive semidefinite Hermitian coefficient matrix $C(\xi)$ characterizing the dephasing environment [31]. Throughout our discussion, we assume $C(\xi) = C(0) + \xi \Delta C$ depends on the sensing target parameter ξ through a simple linear dependence, without loss of generality [32]. Our goal is to build an unbiased estimator for ξ from measurements on some sensor state following time evolution under \mathcal{L}_ξ . To illustrate the idea, we assume a typical scenario where the main resource limiting the measurement accuracy is the total protocol time T (see e.g. [14]), and we are interested in optimizing the amount of extractable information averaged over T in the asymptotically long measurement-time (i.e., $T \rightarrow \infty$) limit. The measurement SNR in this case is upper bounded by the quantum Cramér-Rao bound (CRB) [33]: denoting Δ_ξ as the standard deviation of the estimator, we have $(\xi/\Delta_\xi) \leq \xi \sqrt{T \max_{\hat{\rho}_i, t} \overline{F_Q}(\hat{\rho}_i, \mathcal{L}_\xi; \xi, t)}$, where $\overline{F_Q}(\hat{\rho}_i, \mathcal{L}_\xi; \xi, t)$ is defined as the time-averaged quantum Fisher information (QFI) with respect to ξ , i.e.,

$$\overline{F_Q}(\hat{\rho}_i, \mathcal{L}_\xi; \xi, t) \equiv 8 \lim_{d\xi \rightarrow 0} \frac{1 - \sqrt{F(e^{\mathcal{L}_\xi t} \hat{\rho}_i, e^{\mathcal{L}_{\xi+d\xi} t} \hat{\rho}_i)}}{td\xi^2}. \quad (2)$$

Here, ρ_i is the initial sensor state, and $F(\cdot, \cdot)$ defines the fidelity function between two density operators: $F(\hat{\rho}, \hat{\sigma}) = [\text{Tr}(\sqrt{\sqrt{\hat{\rho}} \hat{\sigma} \sqrt{\hat{\rho}}})]^2$. By convexity of the QFI, we have $\max_t \overline{F_Q}(\hat{\rho}_i, \mathcal{L}_\xi; \xi, t) = \lim_{t \rightarrow 0} \overline{F_Q}(\hat{\rho}_i, \mathcal{L}_\xi; \xi, t)$ for any pure-dephasing Lindbladian (see Appendix A1 for details).

To gain some intuition, we first recall that, in the standard Hamiltonian sensing case, quantum advantage emerges due to an enlarged susceptibility of the sensor GHZ state that is strictly greater than that of any separable sensor state [34]. This mechanism does not directly extend to the Lindblad sensing case: while a GHZ state does decay faster with the dephasing rate scaling as N , such increase in the coherence decay rate also accompanies a degradation

in the directly measured signal. In fact, for sensing dephasing rate due to uncorrelated noise, one can show that there is no net gain in SNR when comparing an entangled state with product-state input [30]. For instance, we may consider the problem of estimating a homogeneous single-qubit dephasing rate, $\mathcal{L}_{\xi, \text{1qb}} = \mathcal{L}_\xi[C(\xi) = \xi]$ in Eq. (1). In this case, the optimal time-averaged QFI for the single-qubit case is obtained by starting in $|+\rangle$:

$$\overline{F_Q}(|+\rangle, \mathcal{L}_{\xi, \text{1qb}}; \xi, t) = \gamma/(2\xi). \quad (3)$$

The optimal QFI with an N -qubit product state is thus given by $N\gamma/(2\xi)$, in accordance with the standard quantum limit (SQL). On the other hand, the optimal sensitivity of measuring ξ with an entangled initial state is saturated by the GHZ state, in which case the maximal time-averaged QFI with respect to ξ can be computed as $N^2\gamma/(2N\xi)$. In this case, the multiqubit GHZ state undergoes a faster dephasing rate $N\xi\gamma$, which has two effects on the time-averaged QFI: the N^2 factor in the numerator stems from a larger noise susceptibility, while the extra N factor in the denominator is due to reduced signal induced by the enhanced dephasing (c.f. Eq. (3)). Thus the entangled state does not create a net quantum advantage for estimating the original single-qubit dephasing parameter ξ . More generally, making use of the no-go theorem in Ref. [30], one can show that the optimal SNR for estimating any single-qubit Markovian and non-Markovian pure-dephasing rates is given by the SQL.

From the above discussion, we see that the standard mechanism for obtaining a quantum advantage in Hamiltonian estimation does not apply to the case of sensing a single-qubit dephasing rate. This motivates us to explore quantum advantage in pure-dephasing Lindbladians with nontrivial spatial correlation, corresponding to the case where the C matrix in Eq. (1) has nonzero off-diagonal elements. Such a scenario can occur if the ensemble of sensor qubits is collectively coupled to a dissipative environment, e.g., in trapped-ion systems when the ions experience dephasing due to phase reference error [35] or their collective coupling to the motional modes [36], or in an atomic array when the atoms are collectively driven by the same laser beam with nontrivial intensity fluctuations [37]. In the context of quantum sensing, as sensor noise measurements can be used to infer the zero-frequency two-point correlation functions of the environmental fluctuations [38], correlated dephasing also naturally arises when sensing fluctuations of a quantum material with nontrivial spatial correlations.

Case study: entanglement advantage in sensing 2-qubit correlated noise.—While the quantum advantage we uncover is generally applicable to a variety of correlated dephasing Lindbladians, to illustrate the basic idea, we first consider the case with 2 qubits subject to a dephasing environment $\mathcal{L}_{\xi,2\text{qb}} = \mathcal{L}_{\xi}[C_{2\text{qb}}(\xi)]$ with nearly maximally correlated noise, given by $[C_{2\text{qb}}(\xi)]_{j\ell} = 1 - \xi(1 - \delta_{j\ell})$ with $\xi \ll 1$. Note that ξ arises in off-diagonal elements of $C(\xi)$, signifying that this parameter is related to *spatial correlation* of the dephasing environment. The eigenvectors of the Lindbladian $\mathcal{L}_{\xi,2\text{qb}}$ are thus given by outer products $|\alpha\rangle\langle\beta|$ spanned by eigenstates of \hat{Z}_1 and \hat{Z}_2 . Here, we use the real vector $\alpha = (\alpha_1, \alpha_2)$ to denote the computational basis states, with $\hat{Z}_j|\alpha\rangle = \alpha_j|\alpha\rangle$. In this case, a generic superposition state of 2 computational basis vectors $|\Psi_{\alpha,\beta}\rangle = (|\alpha\rangle + |\beta\rangle)/\sqrt{2}$ still dephases similarly to the single-qubit case with an effective dephasing rate given by $\gamma_{\alpha,\beta} = \frac{\gamma}{4}(\alpha - \beta)^T C(\alpha - \beta)$ (see e.g. Ref. [39]), so that the time-averaged QFI with respect to ξ using initial state $|\Psi_{\alpha,\beta}\rangle$ is given by $\overline{F}_Q(|\Psi_{\alpha,\beta}\rangle, \mathcal{L}_{\xi,2\text{qb}}; \xi, t) = (\gamma_{\alpha,\beta}/2)(\partial \ln \gamma_{\alpha,\beta}/\partial \xi)^2$. One can thus show that the optimal initial state that maximizes the QFI per protocol time corresponds to the Bell state $|\Psi_{01,10}\rangle = (|01\rangle + |10\rangle)/\sqrt{2}$, which yields $\overline{F}_Q(|\Psi_{01,10}\rangle, \mathcal{L}_{\xi,2\text{qb}}; \xi, t) = \gamma/\xi$.

We now address the question of whether an entanglement advantage exists in the sensing task of estimating ξ in $\mathcal{L}_{\xi,2\text{qb}}$. For this, we need to compute the optimal time-averaged QFI for all separable states, which can be derived analytically as $\max_{|\phi_1\rangle, |\phi_2\rangle, t} \overline{F}_Q(|\phi_1\rangle \otimes |\phi_2\rangle, \mathcal{L}_{\xi,2\text{qb}}; \xi, t) = \gamma/[\xi(2 - \xi)]$ [40]. Noting that $\xi \in [0, 1]$ by definition of the Lindbladian in (1), we have thus shown that using the Bell state $|\Psi_{01,10}\rangle$ generically provides an advantage in estimating ξ parametrizing the 2-qubit Lindbladian for any $\xi < 1$. Further, the ratio between optimal sensitivity using entangled or product states is maximized in the limit $\xi \ll 1$, where we have

$$\lim_{\xi \rightarrow 0} \frac{\max_{\hat{\rho}_i, t} \overline{F}_Q(\hat{\rho}_i, \mathcal{L}_{\xi,2\text{qb}}; \xi, t)}{\max_{|\phi_1\rangle, |\phi_2\rangle, t} \overline{F}_Q(|\phi_1\rangle \otimes |\phi_2\rangle, \mathcal{L}_{\xi,2\text{qb}}; \xi, t)} = 2. \quad (4)$$

We remark that the entanglement enhancement mechanism in Eq. (4) is completely distinct from the case with standard Hamiltonian sensing. More specifically, in contrast to enhancing the Hamiltonian-estimation QFI using a greater response of entangled states to the target Hamiltonian, in the Lindbladian case we instead make use

of the much slower dephasing dynamics of a specific Bell state $|\Psi_{01,10}\rangle$ to enable the entanglement advantage. It is also interesting to note that while it is not physically possible to construct a dephasing Lindbladian where a particular entangled state dephases much faster or slower than all *product* states, as a generic product state will still have nontrivial overlap with the said entangled state, the fact that the QFI monotonically decreases with the entangled state dephasing rate $\gamma_{\alpha\beta}$ means that one can construct an entanglement advantage as long as there exists a unique entangled state that dephases much slower than other eigenstates of the Lindbladian. As we show below, this basic mechanism allows us to construct a class of multiqubit correlated dephasing Lindbladians that hosts a scalable entanglement sensing advantage.

It is worth noting that the entanglement advantage in Eq. (4) persists if the sensing procedure is limited by the total number of measurement runs instead of the probing time. The sensitivity optimized over the number of shots is relevant if the state preparation or detection time is much longer than the time it takes to interrogate the sensing target, which is the case in many current quantum platforms (see, e.g., [12]). In this regime, the minimal measurement uncertainty $\Delta\xi$ over M shots is set by the maximal quantum Fisher information optimized over the protocol time per shot: $\Delta\xi \geq 1/\sqrt{M \max_{\hat{\rho}_i, t} \overline{F}_Q(\hat{\rho}_i, \mathcal{L}_{\xi}; \xi, t)}$. In the $\xi \ll 1$ limit, the maximal QFI per shot over measurement time t is determined by the contribution from $|\Psi_{01,10}\rangle$, and we obtain the same entanglement enhancement as in Eq. (4) (only with the time-averaged QFI \overline{F}_Q replaced by the QFI per shot, F_Q). Hence, the entanglement advantage applies in both the time-averaged and shot-number-averaged regimes. This feature also distinguishes the entanglement advantage in Eq. (4) from the case of channel estimation discussed in Ref. [27].

Generalization to sensing of correlated multiqubit dephasing.—As we discussed, the entanglement enhancement in Eq. (4) crucially relies on the fact that there exists a single entangled state that dephases much slower than any other vectors $|\alpha\rangle\langle\beta|$ in the Lindbladian eigenspectrum (excluding diagonal terms that are conserved in the dephasing dynamics). This inspired us to consider the following correlated dephasing Lindbladian (assume total qubit number N is even):

$$\frac{2}{\gamma} \mathcal{L}_{N\text{qb}} = \xi \mathcal{D}[\hat{Z}_{k=0}] + \sum_{k \neq 0} \mathcal{D}[\hat{Z}_k], \quad (5)$$

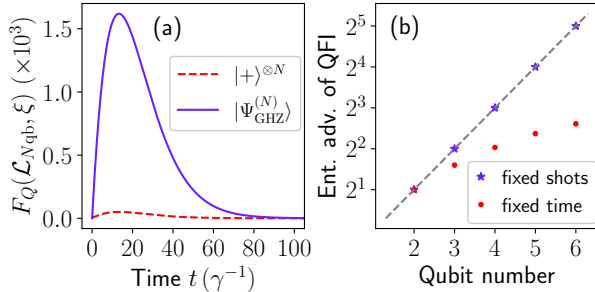


FIG. 1. (a) Numerical calculation of the quantum Fisher information (QFI) $F_Q(\hat{\rho}_i, \mathcal{L}_{N\text{qb}}; \xi, t)$ for estimating ξ in the multiqubit dephasing [see Lindbladian in Eq. (5)] for varying evolution time t per shot, when using the optimal product state $|+\rangle^{\otimes N}$ versus the optimal entangled state $|\Psi_{\text{GHZ}}^{(N)}\rangle$ ($N = 6$). (b) The entanglement advantage, as quantified by the ratio between the optimal QFI using entangled states and that with only product initial states, plotted against qubit number ($N = 2, 3, 4, 5, 6$). Both cases of the optimal QFI with fixed total probing time (red dots) and total number of shots (purple stars) are plotted. The dashed line depicts the analytically predicted entanglement advantage for the maximal QFI optimized over number of shots, 2^{N-1} , which scales exponentially with the qubit number N when fixing the total number of experimental runs, see Eq. (6).

where we define $\hat{Z}_k = (1/\sqrt{N}) \sum_{j=1}^N e^{i\frac{2\pi k}{N}j} \hat{Z}_j$ ($k = 0, 1, \dots, N-1$) for convenience. The corresponding coefficient matrix is given by $[C_{N\text{qb}}(\xi)]_{j\ell} = \delta_{j\ell} - \frac{1-\xi}{N}$. In this case, the optimal QFI can be computed as $\overline{F_Q}(|\Psi_{00\dots,11\dots}\rangle, \mathcal{L}_{\xi, N\text{qb}}; \xi, t) = N\gamma/2\xi$. On the other hand, if we restrict to separable input states $\hat{\rho}_{\text{sep}}$, then the optimal time-averaged QFI can be computed as $\max_{\hat{\rho}_{\text{sep}}, t} \overline{F_Q}(\hat{\rho}_{\text{sep}}, \mathcal{L}_{\xi, N\text{qb}}; \xi, t) = \gamma/2\xi$, giving rise to a factor of \sqrt{N} enhancement in the SNR when using entangled initial states. Here, entanglement enhancement has the same scaling as the standard Hamiltonian estimation case, although, as we discussed, the underlying mechanism is distinct.

An even more striking enhancement emerges if the total number of experimental runs, as opposed to the total protocol time, is constrained in the sensing protocol. In this regime, we care about the optimal QFI per shot, $\max_{\hat{\rho}_i, t} F_Q(\hat{\rho}_i, \mathcal{L}_{\xi}; \xi, t)$. We further focus on the regime with sufficiently small values of ξ , where the lowest nonzero eigenvalue of the Lindbladian in Eq. (5) corresponds to coherence decay of the GHZ-type state $|\Psi_{\text{GHZ}}^{(N)}\rangle = (|0000\dots\rangle + |1111\dots\rangle)/\sqrt{2}$ as $\gamma_{00\dots,11\dots} = 2N\xi\gamma$. Similarly to the 2-qubit case, in the limit $\xi \ll 1/N$, the QFI at times $t \gtrsim 1/\gamma$ is determined by the overlap be-

tween the initial state and $|\Psi_{\text{GHZ}}^{(N)}\rangle$. Consequently, the Lindblad sensing exhibits an entanglement advantage that scales exponentially in the number of qubits, as

$$\xi \rightarrow 0: \frac{\max_{\hat{\rho}_i, t} F_Q(\hat{\rho}_i, \mathcal{L}_{\xi, N\text{qb}}; \xi, t)}{\max_{\hat{\rho}_{\text{sep}}, t} F_Q(\hat{\rho}_{\text{sep}}, \mathcal{L}_{\xi, N\text{qb}}; \xi, t)} = 2^{N-1}, \quad (6)$$

where $\hat{\rho}_{\text{sep}}$ denotes an N -qubit separable state. As shown in Fig. 1, numerical calculation of the entanglement advantage for $\xi = 0.01$ and up to $N = 6$ qubits agrees excellently with the analytical prediction in Eq. (6).

Given the exponentially large enhancement in the sensitivity, it is natural to ask about the dynamical range of ξ in this sensing task. Here, we define dynamical range of our protocol as the regime where the entanglement advantage in Eq. (4) holds; from the above discussion, we see that the dynamical range is given by $\xi_c \sim N/2^{N-1}$. Within this range, the uncertainty of measurement over M runs can be computed from the QFI as

$$\Delta\xi_N(M) = \left[M \max_t F_Q(|\Psi_{\text{GHZ}}^{(N)}\rangle, \mathcal{L}_{\xi, N\text{qb}}; \xi, t) \right]^{-\frac{1}{2}}, \quad (7)$$

which can be straightforwardly shown to scale as $\Delta\xi_N(M) \propto \xi/\sqrt{M}$. We can now view the question of whether ξ lies in the dynamical range as a promise problem: if $\Delta\xi_N(M) < \xi_c$, then the promise holds, otherwise it is broken. If the measurement uncertainty now satisfies $\Delta\xi_N(M) < \xi_c$, then the measurement contributes towards gaining more information about ξ ; conversely, if the measurement uncertainty is greater than the promised value $\Delta\xi_N(M) > \xi_c$, then our measurement does not improve the measurement uncertainty beyond the original promise. It is interesting to note that, in the case of correlated noise sensing, the promise can be explicitly verified by measuring the coherence of the GHZ state after time $t \sim 1/N\xi\gamma$.

We again remark on the drastic distinction between the Lindblad sensing case and the standard Hamiltonian estimation framework: in the standard case of estimating qubit frequency ξ in the Hamiltonian $\hat{H} = \xi \sum_{\ell=1}^N \hat{Z}_\ell$, one can still assume a promise that the frequency is within the dynamical range $\xi \ll 1/N$ such that an entanglement advantage holds; however, this promise cannot be explicitly checked, which limits the utility of the GHZ sensing protocol in practice (without adopting an adaptive measurement scheme, see e.g. [41, 42]).

The Heisenberg limit in Hamiltonian sensing is intrinsically a single-shot limit, whereas the dephasing noise sensing problem is intrinsically limited by shot noise, i.e. in the case of noise sensing, we always have $\Delta\xi \sim T^{-\frac{1}{2}}$ or $M^{-\frac{1}{2}}$, depending on whether we constrain the total protocol time or the number of shots. In the Hamiltonian case, there is a fundamental tradeoff between the achievable sensitivity versus the number of shots implemented; however, in Lindblad noise sensing, increasing the number of shots can lead to a nontrivial enhancement in the protocol sensitivity.

Application: estimating spatial correlations in quantum materials.—The collective dephasing dynamics in Eq. (5) naturally arise when we use an array of qubits to probe noise properties of a spatially extended target. More specifically, we can generally use a system-environment model to describe the microscopic interaction giving rise to Eq. (5), where the total setup evolves under the Hamiltonian $\hat{H}_{\text{tot}} = \frac{1}{2} \sum_{\ell=1}^N (\omega_{\ell} + \hat{B}_{\ell}) \hat{Z}_{\ell} + \hat{H}_{\text{env}}$. In the limit the environment acts as a Gaussian and Markovian bath on the qubits, the dephasing coefficient matrix in Eq. (1) is directly related to correlation functions of the environmental operators as

$$C_{j\ell} = \frac{2}{\gamma} \lim_{\omega \rightarrow 0} \mathcal{S}_{j\ell}[\omega], \quad (8)$$

where $\mathcal{S}_{j\ell}[\omega] = \frac{1}{2} \int_{-\infty}^{\infty} \langle \{\hat{B}_j(s), \hat{B}_{\ell}(0)\} \rangle e^{i\omega s} ds$ are the noise spectral densities of \hat{B}_j , with $\hat{B}_j(s) \equiv e^{i\hat{H}_{\text{env}}s} \hat{B}_j e^{-i\hat{H}_{\text{env}}s}$ denoting the interaction-picture environmental noise operators. We note that Eq. (8) also applies if the environment consists of classical stochastic quantities, in which case $\mathcal{S}_{j\ell}[\omega]$ correspond to the noise spectral densities of those classical fluctuations.

Our protocol for sensing dephasing Lindbladians can thus be used to extract information about zero-frequency noise spectral densities of the environment, i.e., the sensing target. By applying standard dynamical decoupling or spin-locking sequences, we can also extend Eq. (8) to measuring spectral properties of the environmental noise at nonzero frequencies [43, 44]. Intriguingly, Eq. (5) naturally arises if the environment is fully scrambled in almost all the degrees of freedom, except the center-of-mass (i.e., $k = 0$) mode. The latter may happen if the sensing target is subject to conservation laws of momentum in the center-of-mass mode.

Discussion and outlook.—In this work, we uncover a new mechanism for obtaining entanglement advantage in sensing spatially-correlated Markovian noise. When the total protocol time is fixed, we find a

Heisenberg-type scaling in the time-averaged QFI for estimating a small deviation of sensor dynamics from maximally correlated dephasing; such an entanglement advantage even scales exponentially when the total number of experimental runs is constrained. While super-Heisenberg scaling has been explored in the context of Hamiltonian sensing as well, all known examples of larger-than-Heisenberg entanglement advantage involves a sensor Hamiltonian that can generate entanglement during time evolution [1, 45, 46]. In contrast, the correlated dephasing dynamics we consider in this work cannot create any entanglement.

Another related type of sensing tasks involves channel estimation. In the latter context, Ref. [29] showed that channel parameter estimation can have at best Heisenberg-type entanglement advantage in terms of the number of channel uses. An intriguing direction for future investigation is whether an exponential advantage emerges in more general Lindbladian sensing problems.

As mentioned, our framework [c.f. Eq. (8)] can be directly generalized to study non-Markovian noise of the environment, with the help of standard qubit noise spectroscopy techniques (see, e.g., [47–49]). An outstanding challenge is whether one can obtain a quantum advantage in probing a non-Markovian environment. While we do not expect any entanglement-based enhancement in probing spatially uncorrelated dephasing noise, finding the optimal strategy to reconstruct environmental noise properties with both nontrivial spatial and temporal correlations remains an open question. It is also interesting to explore possible extensions of our results to multi-parameter estimation. Previous works have shown that entanglement can enable an exponential advantage in the number of samples required to learn Pauli channel parameters (see e.g. Refs. [50, 51]). It is thus intriguing to ask whether our results can be used to enhance learning algorithms for general non-Pauli dephasing channels. We leave this to future work.

Acknowledgments.—We thank Lorenza Viola and Gideon Lee for helpful discussions. J.B. acknowledges support from the Harvard Quantum Initiative. J.B. and A.V.G. were supported in part by AFOSR MURI, DARPA SAVaNT ADVENT, NSF STAQ program, NSF QLCI (award No. OMA-2120757), DoE ASCR Quantum Testbed Pathfinder program (awards No. DE-SC0019040 and No. DE-SC0024220), and DoE ASCR Accelerated Research in Quantum Computing program (award No. DE-SC0020312). A.J.B. acknowledges support from the NRC Research Associateship Program at NIST.

Support is also acknowledged from the U.S. Department of Energy, Office of Science, National Quan-

tum Information Science Research Centers, Quantum Systems Accelerator.

-
- [1] V. Giovannetti, S. Lloyd, and L. Maccone, Advances in quantum metrology, *Nat. Photonics* **5**, 222–229 (2011).
- [2] C. L. Degen, F. Reinhard, and P. Cappellaro, Quantum sensing, *Rev. Mod. Phys.* **89**, 035002 (2017).
- [3] L. Pezzè, A. Smerzi, M. K. Oberthaler, R. Schmied, and P. Treutlein, Quantum metrology with nonclassical states of atomic ensembles, *Rev. Mod. Phys.* **90**, 035005 (2018).
- [4] S. Pirandola, B. R. Bardhan, T. Gehring, C. Weedbrook, and S. Lloyd, Advances in photonic quantum sensing, *Nat. Photonics* **12**, 724–733 (2018).
- [5] T. Nagata, R. Okamoto, J. L. O’Brien, K. Sasaki, and S. Takeuchi, Beating the Standard Quantum Limit with Four-Entangled Photons, *Science* **316**, 726 (2007).
- [6] B. L. Higgins, D. W. Berry, S. D. Bartlett, H. M. Wiseman, and G. J. Pryde, Entanglement-free Heisenberg-limited phase estimation, *Nature* **450**, 393–396 (2007).
- [7] W. Wang, Y. Wu, Y. Ma, W. Cai, L. Hu, X. Mu, Y. Xu, Z.-J. Chen, H. Wang, Y. P. Song, *et al.*, Heisenberg-limited single-mode quantum metrology in a superconducting circuit, *Nat. Commun.* **10**, 4382 (2019).
- [8] L.-Z. Liu, Y.-Z. Zhang, Z.-D. Li, R. Zhang, X.-F. Yin, Y.-Y. Fei, L. Li, N.-L. Liu, F. Xu, Y.-A. Chen, *et al.*, Distributed quantum phase estimation with entangled photons, *Nat. Photonics* **15**, 137–142 (2020).
- [9] J. A. H. Nielsen, J. S. Neergaard-Nielsen, T. Gehring, and U. L. Andersen, Deterministic Quantum Phase Estimation beyond N00N States, *Phys. Rev. Lett.* **130**, 123603 (2023).
- [10] A. D. Ludlow, M. M. Boyd, J. Ye, E. Peik, and P. O. Schmidt, Optical atomic clocks, *Rev. Mod. Phys.* **87**, 637 (2015).
- [11] J. M. Robinson, M. Miklos, Y. M. Tso, C. J. Kennedy, T. Bothwell, D. Kedar, J. K. Thompson, and J. Ye, Direct comparison of two spin-squeezed optical clock ensembles at the 10^{-17} level, *Nat. Phys.* **20**, 208–213 (2024).
- [12] S. C. Burd, R. Srinivas, J. J. Bollinger, A. C. Wilson, D. J. Wineland, D. Leibfried, D. H. Slichter, and D. T. C. Allcock, Quantum amplification of mechanical oscillator motion, *Science* **364**, 1163 (2019).
- [13] A. Facon, E.-K. Dietsche, D. Grosso, S. Haroche, J.-M. Raimond, M. Brune, and S. Gleyzes, A sensitive electrometer based on a Rydberg atom in a Schrödinger-cat state, *Nature* **535**, 262–265 (2016).
- [14] K. A. Gilmore, M. Affolter, R. J. Lewis-Swan, D. Barberena, E. Jordan, A. M. Rey, and J. J. Bollinger, Quantum-enhanced sensing of displacements and electric fields with two-dimensional trapped-ion crystals, *Science* **373**, 673 (2021).
- [15] J. A. Jones, S. D. Karlen, J. Fitzsimons, A. Ardavan, S. C. Benjamin, G. A. D. Briggs, and J. J. L. Morton, Magnetic Field Sensing Beyond the Standard Quantum Limit Using 10-Spin NOON States, *Science* **324**, 1166 (2009).
- [16] W. Muessel, H. Strobel, D. Linnemann, D. B. Hume, and M. K. Oberthaler, Scalable Spin Squeezing for Quantum-Enhanced Magnetometry with Bose-Einstein Condensates, *Phys. Rev. Lett.* **113**, 103004 (2014).
- [17] D. Ganapathy *et al.* (LIGO O4 Detector Collaboration), Broadband Quantum Enhancement of the LIGO Detectors with Frequency-Dependent Squeezing, *Phys. Rev. X* **13**, 041021 (2023).
- [18] V. Giovannetti, S. Lloyd, and L. Maccone, Quantum-Enhanced Measurements: Beating the Standard Quantum Limit, *Science* **306**, 1330–1336 (2004).
- [19] S. F. Huelga, C. Macchiavello, T. Pellizzari, A. K. Ekert, M. B. Plenio, and J. I. Cirac, Improvement of Frequency Standards with Quantum Entanglement, *Phys. Rev. Lett.* **79**, 3865 (1997).
- [20] B. M. Escher, R. L. de Matos Filho, and L. Davidovich, General framework for estimating the ultimate precision limit in noisy quantum-enhanced metrology, *Nat. Phys.* **7**, 406 (2011).
- [21] R. Demkowicz-Dobrzański, J. Kołodyński, and M. Guţă, The elusive Heisenberg limit in quantum-enhanced metrology, *Nat. Commun.* **3**, 1063 (2012).
- [22] W. Zhong, Z. Sun, J. Ma, X. Wang, and F. Nori, Fisher information under decoherence in Bloch representation, *Phys. Rev. A* **87**, 022337 (2013).
- [23] J. F. Haase, A. Smirne, J. Kołodyński, R. Demkowicz-Dobrzański, and S. F. Huelga, Fundamental limits to frequency estimation: a comprehensive microscopic perspective, *New J. Phys.* **20**, 053009 (2018).
- [24] J. Jeske, J. H. Cole, and S. F. Huelga, Quantum metrology subject to spatially correlated Markovian noise: restoring the Heisenberg limit, *New J. Phys.* **16**, 073039 (2014).
- [25] R. Demkowicz-Dobrzański, J. Czajkowski, and P. Sekatski, Adaptive Quantum Metrology under General Markovian Noise, *Phys. Rev. X* **7**, 041009 (2017).
- [26] S. Zhou, M. Zhang, J. Preskill, and L. Jiang, Achieving the Heisenberg limit in quantum metrology using quantum error correction, *Nat. Commun.* **9**, 78 (2018).

- [27] S. Boixo and A. Monras, Operational Interpretation for Global Multipartite Entanglement, *Phys. Rev. Lett.* **100**, 100503 (2008).
- [28] S. P. Wolski, D. Lachance-Quirion, Y. Tabuchi, S. Kono, A. Noguchi, K. Usami, and Y. Nakamura, Dissipation-Based Quantum Sensing of Magnons with a Superconducting Qubit, *Phys. Rev. Lett.* **125**, 117701 (2020).
- [29] S. Kurdzialek, W. Górecki, F. Albarelli, and R. Demkowicz-Dobrzański, Using Adaptiveness and Causal Superpositions Against Noise in Quantum Metrology, *Phys. Rev. Lett.* **131**, 090801 (2023).
- [30] S. Pirandola and C. Lupo, Ultimate Precision of Adaptive Noise Estimation, *Phys. Rev. Lett.* **118**, 100502 (2017).
- [31] J. H. Reina, L. Quiroga, and N. F. Johnson, Decoherence of quantum registers, *Phys. Rev. A* **65**, 032326 (2002).
- [32] If $C(\xi)$ has a more generic functional dependence on ξ , then in the context of single-parameter estimation, we can always linearize the function $C(\xi)$ in the vicinity of the estimated value of the parameter ξ_0 as $C(\xi) \simeq C(\xi_0) + (\xi - \xi_0)\partial_\xi C(\xi_0)$, which would lead to a linear dependence of the dephasing coefficient matrix on ξ .
- [33] S. L. Braunstein and C. M. Caves, Statistical distance and the geometry of quantum states, *Phys. Rev. Lett.* **72**, 3439 (1994).
- [34] D. J. Wineland, J. J. Bollinger, W. M. Itano, and D. J. Heinzen, Squeezed atomic states and projection noise in spectroscopy, *Phys. Rev. A* **50**, 67 (1994).
- [35] T. Monz, P. Schindler, J. T. Barreiro, M. Chwalla, D. Nigg, W. A. Coish, M. Harlander, W. Hänsel, M. Hennrich, and R. Blatt, 14-Qubit Entanglement: Creation and Coherence, *Phys. Rev. Lett.* **106**, 130506 (2011).
- [36] M. Brownnutt, M. Kumph, P. Rabl, and R. Blatt, Ion-trap measurements of electric-field noise near surfaces, *Rev. Mod. Phys.* **87**, 1419 (2015).
- [37] A. L. Shaw, Z. Chen, J. Choi, D. K. Mark, P. Scholl, R. Finkelstein, A. Elben, S. Choi, and M. Endres, Benchmarking highly entangled states on a 60-atom analogue quantum simulator, *Nature* **628**, 71–77 (2024).
- [38] R. Klesse and S. Frank, Quantum Error Correction in Spatially Correlated Quantum Noise, *Phys. Rev. Lett.* **95**, 230503 (2005).
- [39] A. Seif, M. Hafezi, and Y.-K. Liu, Compressed Sensing Measurement of Long-Range Correlated Noise (2021), [arXiv:2105.12589](https://arxiv.org/abs/2105.12589) [quant-ph].
- [40] Note that the maximal time-averaged QFI over all separable states can always be saturated by a product initial state, by convexity of the quantum Fisher information.
- [41] V. Bužek, R. Derka, and S. Massar, Optimal Quantum Clocks, *Phys. Rev. Lett.* **82**, 2207 (1999).
- [42] E. M. Kessler, P. Kómár, M. Bishof, L. Jiang, A. S. Sørensen, J. Ye, and M. D. Lukin, Heisenberg-Limited Atom Clocks Based on Entangled Qubits, *Phys. Rev. Lett.* **112**, 190403 (2014).
- [43] T. Yuge, S. Sasaki, and Y. Hirayama, Measurement of the Noise Spectrum Using a Multiple-Pulse Sequence, *Phys. Rev. Lett.* **107**, 170504 (2011).
- [44] G. A. Álvarez and D. Suter, Measuring the Spectrum of Colored Noise by Dynamical Decoupling, *Phys. Rev. Lett.* **107**, 230501 (2011).
- [45] S. Boixo, S. T. Flammia, C. M. Caves, and J. Geremia, Generalized Limits for Single-Parameter Quantum Estimation, *Phys. Rev. Lett.* **98**, 090401 (2007).
- [46] S. M. Roy and S. L. Braunstein, Exponentially Enhanced Quantum Metrology, *Phys. Rev. Lett.* **100**, 220501 (2008).
- [47] J. Bylander, S. Gustavsson, F. Yan, F. Yoshihara, K. Harrabi, G. Fitch, D. G. Cory, Y. Nakamura, J.-S. Tsai, and W. D. Oliver, Noise spectroscopy through dynamical decoupling with a superconducting flux qubit, *Nat. Phys.* **7**, 565–570 (2011).
- [48] G. A. Paz-Silva, L. M. Norris, and L. Viola, Multiqubit spectroscopy of Gaussian quantum noise, *Phys. Rev. A* **95**, 022121 (2017).
- [49] U. von Lüpké, F. Beaudoin, L. M. Norris, Y. Sung, R. Winik, J. Y. Qiu, M. Kjaergaard, D. Kim, J. Yoder, S. Gustavsson, *et al.*, Two-Qubit Spectroscopy of Spatiotemporally Correlated Quantum Noise in Superconducting Qubits, *PRX Quantum* **1**, 010305 (2020).
- [50] S. Chen, C. Oh, S. Zhou, H.-Y. Huang, and L. Jiang, Tight Bounds on Pauli Channel Learning without Entanglement, *Phys. Rev. Lett.* **132**, 180805 (2024).
- [51] A. Seif, S. Chen, S. Majumder, H. Liao, D. S. Wang, M. Malekakhlagh, A. Javadi-Abhari, L. Jiang, and Z. K. Mineev, Entanglement-enhanced learning of quantum processes at scale (2024), [arXiv:2408.03376](https://arxiv.org/abs/2408.03376) [quant-ph].

Appendix A: Explicit derivation of optimal time-averaged QFI for pure-dephasing Lindbladians

In this Appendix, we provide more details on the calculation of the optimal time-averaged QFI in estimating a generic parameter ξ of Lindbladians \mathcal{L}_ξ involving purely dissipative dynamics, and, as specific examples, reproduce the analytical results presented in the main text for various pure-dephasing Lindbladians.

1. General formula

In Eq. (2) in the main text, we introduce the time-averaged QFI $\overline{F_Q}(\hat{\rho}_i, \mathcal{L}_\xi; \xi, t)$, which quantifies the maximal information extractable in ξ by measuring

the time evolution of $\hat{\rho}_i$ under \mathcal{L}_ξ for time t . This quantity can be formally defined using the fidelity function, or equivalently the Bures metric d_{Bures} , as

$$\begin{aligned} \overline{F_Q}(\hat{\rho}_i, \mathcal{L}_\xi; \xi, t) &\equiv 8 \frac{1 - \sqrt{F(e^{\mathcal{L}_\xi t} \hat{\rho}_i, e^{\mathcal{L}_{\xi+d\xi} t} \hat{\rho}_i)}}{td\xi^2} \\ &= 4 \frac{d_{\text{Bures}}^2(e^{\mathcal{L}_\xi t} \hat{\rho}_i, e^{\mathcal{L}_{\xi+d\xi} t} \hat{\rho}_i)}{td\xi^2}. \end{aligned} \quad (\text{A1})$$

When the total protocol time is fixed, the optimal sensitivity is given by the time-averaged QFI maximized over all initial state $\hat{\rho}_i$ and evolution time t , as (see main text)

$$\Delta\xi \geq 1/\sqrt{T \max_{\hat{\rho}_i, t} \overline{F_Q}(\hat{\rho}_i, \mathcal{L}_\xi; \xi, t)}, \quad (\text{A2})$$

where $\Delta\xi$ denotes the standard error of the estimated ξ in the long-measurement-time limit.

We now prove a general result that allows us to compute the optimal sensitivity analytically:

$$\begin{aligned} &\max_t \frac{d_{\text{Bures}}^2(e^{\mathcal{L}_\xi t} \hat{\rho}_i, e^{\mathcal{L}_{\xi+d\xi} t} \hat{\rho}_i)}{td\xi^2} \\ &= \lim_{t \rightarrow 0} \left(\frac{d_{\text{Bures}}^2(e^{\mathcal{L}_\xi t} \hat{\rho}_i, e^{\mathcal{L}_{\xi+d\xi} t} \hat{\rho}_i)}{td\xi^2} \right). \end{aligned} \quad (\text{A3})$$

In order to prove this equality, we first formally divide the total protocol time t into M equal intervals such that t/M is much shorter than all relevant time scales in the system. We thus have

$$\begin{aligned} &\lim_{M \rightarrow +\infty} \left(M \max_{\hat{\rho}_i} \frac{d_{\text{Bures}}^2(e^{\frac{t}{M} \mathcal{L}_\xi} \hat{\rho}_i, e^{\frac{t}{M} \mathcal{L}_{\xi+d\xi}} \hat{\rho}_i)}{td\xi^2} \right) \\ &= \lim_{\tau \rightarrow 0} \left(\max_{\hat{\rho}_i} \frac{d_{\text{Bures}}^2(e^{\tau \mathcal{L}_\xi} \hat{\rho}_i, e^{\tau \mathcal{L}_{\xi+d\xi}} \hat{\rho}_i)}{\tau d\xi^2} \right). \end{aligned} \quad (\text{A4})$$

We now make use of the following inequality that relates the Bures distance between states evolved under two generic completely positive trace-preserving (CPTP) maps \mathcal{C}_A and \mathcal{C}_B and the corresponding distance metric for when applying them for M times:

$$\frac{d_{\text{Bures}}^2(\mathcal{C}_A^M \hat{\rho}_i, \mathcal{C}_B^M \hat{\rho}_i)}{M} \leq d_{\text{Bures}}^2(\mathcal{C}_A \hat{\rho}_i, \mathcal{C}_B \hat{\rho}_i), \quad (\text{A5})$$

where M is an arbitrary positive integer. This can be proved via the convexity of the Bures distance, which ensures that the following inequality holds:

$$\begin{aligned} &d_{\text{Bures}}^2(\mathcal{C}_A^M \hat{\rho}_i, \mathcal{C}_B^M \hat{\rho}_i) \\ &\leq d_{\text{Bures}}^2(\mathcal{C}_A^M \hat{\rho}_i, \mathcal{C}_B[\mathcal{C}_A^{M-1} \hat{\rho}_i]) + d_{\text{Bures}}^2(\mathcal{C}_B[\mathcal{C}_A^{M-1} \hat{\rho}_i], \mathcal{C}_B^M \hat{\rho}_i) \\ &\leq d_{\text{Bures}}^2(\mathcal{C}_A \hat{\rho}_i, \mathcal{C}_B \hat{\rho}_i) + d_{\text{Bures}}^2(\mathcal{C}_A^{M-1} \hat{\rho}_i, \mathcal{C}_B^{M-1} \hat{\rho}_i). \end{aligned} \quad (\text{A6})$$

We can apply Eq. (A6) recursively to show that the following holds

$$\begin{aligned} &d_{\text{Bures}}^2(\mathcal{C}_A^M \hat{\rho}_i, \mathcal{C}_B^M \hat{\rho}_i) \\ &\leq d_{\text{Bures}}^2(\mathcal{C}_A \hat{\rho}_i, \mathcal{C}_B \hat{\rho}_i) + d_{\text{Bures}}^2(\mathcal{C}_A^{M-1} \hat{\rho}_i, \mathcal{C}_B^{M-1} \hat{\rho}_i) \\ &\leq \dots \leq M d_{\text{Bures}}^2(\mathcal{C}_A \hat{\rho}_i, \mathcal{C}_B \hat{\rho}_i), \end{aligned} \quad (\text{A7})$$

which proves Eq. (A5).

Applying Eq. (A5) to the choice of channels $\mathcal{C}_A = e^{\frac{t}{M} \mathcal{L}_\xi}$ and $\mathcal{C}_B = e^{\frac{t}{M} \mathcal{L}_{\xi+d\xi}}$, we thus have

$$\begin{aligned} &\max_{\hat{\rho}_i, t} \frac{d_{\text{Bures}}^2(e^{\mathcal{L}_\xi t} \hat{\rho}_i, e^{\mathcal{L}_{\xi+d\xi} t} \hat{\rho}_i)}{td\xi^2} \\ &\leq \frac{M d_{\text{Bures}}^2(e^{\frac{t}{M} \mathcal{L}_\xi} \hat{\rho}_i, e^{\frac{t}{M} \mathcal{L}_{\xi+d\xi}} \hat{\rho}_i)}{td\xi^2}. \end{aligned} \quad (\text{A8})$$

Taking the limit $M \rightarrow \infty$, and noting that the maximal time-averaged QFI always occurs at a finite time (since the dynamics is purely dissipative), we can now derive an upper bound on the time-averaged QFI as

$$\begin{aligned} &\max_{\hat{\rho}_i, t} \frac{d_{\text{Bures}}^2(e^{\mathcal{L}_\xi t} \hat{\rho}_i, e^{\mathcal{L}_{\xi+d\xi} t} \hat{\rho}_i)}{td\xi^2} \\ &\leq \lim_{M \rightarrow +\infty} \left(\max_{\hat{\rho}_i, t} \frac{M d_{\text{Bures}}^2(e^{\frac{t}{M} \mathcal{L}_\xi} \hat{\rho}_i, e^{\frac{t}{M} \mathcal{L}_{\xi+d\xi}} \hat{\rho}_i)}{td\xi^2} \right) \\ &= \lim_{t \rightarrow 0} \left(\max_{\hat{\rho}_i} \frac{d_{\text{Bures}}^2(e^{\mathcal{L}_\xi t} \hat{\rho}_i, e^{\mathcal{L}_{\xi+d\xi} t} \hat{\rho}_i)}{td\xi^2} \right). \end{aligned} \quad (\text{A9})$$

One can straightforwardly show that the upper bound in above inequality can be saturated by constantly resetting the sensor quantum system and repeating the measurement for a large number of times. Hence, when constraining the total protocol time T , the optimized Fisher information is given by

$$\begin{aligned} &T \max_{\hat{\rho}_i, t} \overline{F_Q}(\hat{\rho}_i, \mathcal{L}_\xi; \xi, t) \\ &= 4T \max_{\hat{\rho}_i, t} \frac{d_{\text{Bures}}^2(e^{\mathcal{L}_\xi t} \hat{\rho}_i, e^{\mathcal{L}_{\xi+d\xi} t} \hat{\rho}_i)}{td\xi^2} \\ &= 4T \lim_{t \rightarrow 0} \left(\max_{\hat{\rho}_i} \frac{d_{\text{Bures}}^2(e^{\mathcal{L}_\xi t} \hat{\rho}_i, e^{\mathcal{L}_{\xi+d\xi} t} \hat{\rho}_i)}{td\xi^2} \right) \\ &= T \lim_{t \rightarrow 0} \left(\max_{\hat{\rho}_i} \overline{F_Q}(\hat{\rho}_i, \mathcal{L}_\xi; \xi, t) \right). \end{aligned} \quad (\text{A10})$$

We can now use Eq. (A10) to explicitly derive the optimal QFI when the Lindbladian \mathcal{L}_ξ is a pure-dephasing-type Lindbladian characterized by the positive semi-definite matrix $C(\xi)$:

$$\mathcal{L}_\xi \hat{\rho} \frac{\gamma}{2} \sum_{j,\ell=1}^n c_{j\ell}(\xi) (\hat{Z}_j \hat{\rho} \hat{Z}_j - \frac{1}{2} \{\hat{Z}_j \hat{Z}_\ell, \hat{\rho}\}). \quad (\text{A11})$$

More concretely, we assume $C(\xi) = C_0 + \xi\Delta C$, and the dephasing coefficient matrix at $\xi = 0$ can be diagonalized as $C_0 = \sum_\ell \epsilon_\ell \boldsymbol{\eta}_\ell \boldsymbol{\eta}_\ell^\dagger$, where $\boldsymbol{\eta}_\ell$ denotes the n -dimensional column eigenvectors of C_0 . We can now explicitly compute the rate of change of QFI in the $t \rightarrow 0$ limit with respect to ξ in terms of the symmetric logarithmic derivative \mathcal{R}^{-1} [33] as

$$\begin{aligned}
& \lim_{t \rightarrow 0} \left(\max_{\hat{\rho}_i} \overline{F_Q}(\hat{\rho}_i, \mathcal{L}_\xi; \xi, t) \right) \\
&= \lim_{t \rightarrow 0} \left[\text{tr}(\delta \mathcal{L}(e^{\mathcal{L}_\xi t} \hat{\rho}_i) \mathcal{R}_{e^{\mathcal{L}_\xi t} \hat{\rho}_i}^{-1} (\delta \mathcal{L}(e^{\mathcal{L}_\xi t} \hat{\rho}_i))) t \right] \\
&= \frac{\gamma}{2} \sum_j \frac{(\langle \psi_\ell | \sum_{a,b=1}^n \Delta c_{ab}(\xi_0) \hat{Z}_b \hat{\rho} \hat{Z}_a | \psi_\ell \rangle)^2}{\epsilon_\ell (\langle \psi_\ell | \psi_\ell \rangle)^3} \\
&+ \gamma \sum_{j \neq \ell} \frac{|\langle \psi_j | \sum_{a,b=1}^n \Delta c_{ab}(\xi_0) \hat{Z}_b \hat{\rho} \hat{Z}_a | \psi_\ell \rangle|^2}{(\epsilon_\ell \langle \psi_\ell | \psi_\ell \rangle + \epsilon_j \langle \psi_\ell | \psi_\ell \rangle) (\langle \psi_\ell | \psi_\ell \rangle \langle \psi_j | \psi_j \rangle)}, \tag{A12}
\end{aligned}$$

where $|\psi_\ell\rangle = \sum_j (\boldsymbol{\eta}_\ell e_j^\dagger) \hat{Z}_j |\phi_i\rangle$. Intuitively, $|\psi_\ell\rangle$ denotes the quantum state conditioned on the system undergoing a quantum jump at the beginning of the evolution corresponding to $\boldsymbol{\eta}_\ell$ in the quantum-jump trajectory picture.

2. Case study: 2-qubit Lindbladian $\mathcal{L}_{\xi, 2\text{qb}}$ and multiqubit Lindbladian $\mathcal{L}_{\xi, N\text{qb}}$

We can use Eq. (A12) to calculate the optimal QFI when constraining the total protocol time.

In the case of the multiqubit dephasing Lindbladian $\mathcal{L}_{N\text{qb}}$ discussed in the main text, the coefficient matrix is given by $C_{N\text{qb}}(\xi) = \mathbb{I}_N - \frac{1-\xi}{N} \sum_{j,\ell} |j\rangle\langle\ell|$. We thus obtain the optimal QFI when using only separable input states $\hat{\rho}_{\text{sep}}$ and the optimal QFI over all quantum states as

$$\max_{\hat{\rho}_i \in \hat{\rho}_{\text{sep}}; t} \overline{F_Q}(\hat{\rho}_i, \mathcal{L}_{\xi, N\text{qb}}; \xi, t) = \frac{\gamma}{2} \frac{1}{\xi}, \tag{A13}$$

$$\max_{\hat{\rho}_i; t} \overline{F_Q}(\hat{\rho}_i, \mathcal{L}_{\xi, N\text{qb}}; \xi, t) = \frac{\gamma}{2} \frac{N}{\xi}. \tag{A14}$$

We see that, in this case, using an entangled state leads to a factor- N enhancement in the QFI, which is the same scaling as the standard Heisenberg limit, although the QFI does not have Heisenberg scaling with respect to total measurement time.